

Prediction of Wind-Induced Ventilation for Livestock Housing

Y. Choinière^a, H. Tanaka^b, J.A. Munroe^c and A. Suchorski-Tremblay^a

^aEng. Res. Unit, Res. Mgmt Branch, Alfred College of Agr. and Food Tech., Alfred, Ontario, Canada, K0B 1A0

^bUniversity of Ottawa, Civil Eng. Dept., Ottawa, Ontario, Canada, K1N 6N5

^cAnimal Res. Centre, Agriculture Canada, Ottawa, Ontario, Canada, K1A 0C6

INTRODUCTION

During hot weather, naturally ventilated buildings depend mainly on wind forces to move air through the building. Livestock are affected by the interior airflow patterns which can be closely associated with the distribution and magnitude of inflows and outflows through the building periphery. The airflow effects of structural parameters, such as size and type of ridge, end wall, and sidewall openings can be analyzed using pressure coefficient data. With the pressure difference method, the total ventilation rate, air inlet and outlet zones, as well as the magnitude of pressure differences between inside and outside can be determined based on measurements of the pressure coefficients around a scale model in a wind tunnel. In addition, measurement of the internal pressure coefficient ($C_{p_{in}}$) at various locations inside the model is used to verify the calculated $C_{p_{in}}$. To better understand scale modeling techniques for natural ventilation of low-rise buildings, it was decided to investigate differences obtained in measurements using either a sealed or an open model with large wall porosities and different roof openings.

OBJECTIVES

The objectives of this study were to use a 1:20 scale model of a low-rise, naturally ventilated building in a wind tunnel to measure external and internal pressure coefficients. These coefficients would then be used to:

- 1 - Visualize the effect of various structural configurations on the variation of the external pressure coefficients, C_{ps} , around the building and on the variations of the internal pressure coefficients, $C_{p_{in}}$ s.
- 2 - Identify the airflow inlet and outlet zones and the relative magnitude of ΔC_{ps} and Q_i over each opening area.
- 3 - Calculate the ventilation rate coefficients, C_{Q10} .
- 4 - Compare the ΔC_{ps} distributions and the C_{Q10} values of an open versus sealed scale model.

METHODS AND PROCEDURES

Different scale models have been used for the purpose of flow visualization and airflow measurements in natural ventilation studies using geometric 1:10 to 1:25

scale models [1-5]. The effect of scaling on the interior velocity and natural ventilation measurements has been discussed.

Scale model description

Figures 1 and 2 present the dimensions of the scale model and the pressure tap locations used for the sealed model and the open model. This 1:20 scale model represents a typical dairy or swine, gable roof barn, 12.2 m wide by 24.4 m long, having 2.7 m high sidewalls, a roof with a 4/12 slope, and a 300 mm eave overhang. There are no interior partitions and the ceiling has the same slope as the roof. Both figures show 10 windows on both sidewalls and 2 windows on both end walls. In the open model, two sizes of sidewall windows were tested, one having a dimension of 110 mm x 40 mm which simulated a continuous opening of 800 mm, the other having a dimension of 110 mm x 55 mm which simulated a continuous opening of 1100 mm. The former size of sidewall window was equal to 27% of the sidewall surface and the latter to 37%. A vertical support was left between each window, which represented the building's structural posts, spaced 2.4 m apart. The size of each end wall window was 60 mm x 100 mm.

Three roof opening configurations were tested. As shown in Figs. 1 and 2, four chimneys of 26 mm x 26 mm (interior dimensions) (520 mm x 520 mm, full scale) were built in order to respect the recommended minimum ridge opening [6,7]. Also, continuous ridge openings of 7.5 mm and 20 mm (150 mm and 400 mm, full scale) were built because they are commonly used in agricultural buildings [4,6].

Wind tunnel facilities

The 2 x 3 m low speed wind tunnel of the National Research Council of Canada (NRCC), located in Ottawa, Ontario, was the testing site for this study.

The simulation of an isothermal boundary layer flow representative of the wind for the lower neutral atmospheric surface was performed in order to study the wind loading over low-rise buildings [3-5,8]. The necessary conditions were: undistorted scaling of the model geometry, vertical profile of wind speed, turbulence intensity, turbulence integral scale, and small blockage of the wind tunnel.

For the NRCC wind tunnel, spires were designed for the simulation of natural wind. The spires were prepared in order to produce a 350 mm thick boundary layer according to the power law equation with an $\alpha = 0.173$ representing open country. Compromises for the simulation of the turbulence intensity, turbulence integral scale and blockage effect were also studied [3,4].

For the present study, the reference wind speed was about 16 m/s (freestream wind speed was 20 m/s) giving a Re of 6.5×10^4 , based on L_c = width of the building. The selection of a scale of 1:20 and a freestream wind speed of 20 m/s was appropriate with respect to the recommended minimum Re of 2×10^4 [5] which should be maintained for natural ventilation studies.

Pressure difference method

The pressure coefficients were measured for both open and closed models according to the standard procedure and the ventilation rates were calculated using the pressure difference method [3,8-10]. Numerous authors [8,10,11] have presented a complete procedure for calculating natural ventilation airflows in low-rise buildings assuming that: 1 - there was no stack effect, 2 - no pressure drop inside the building

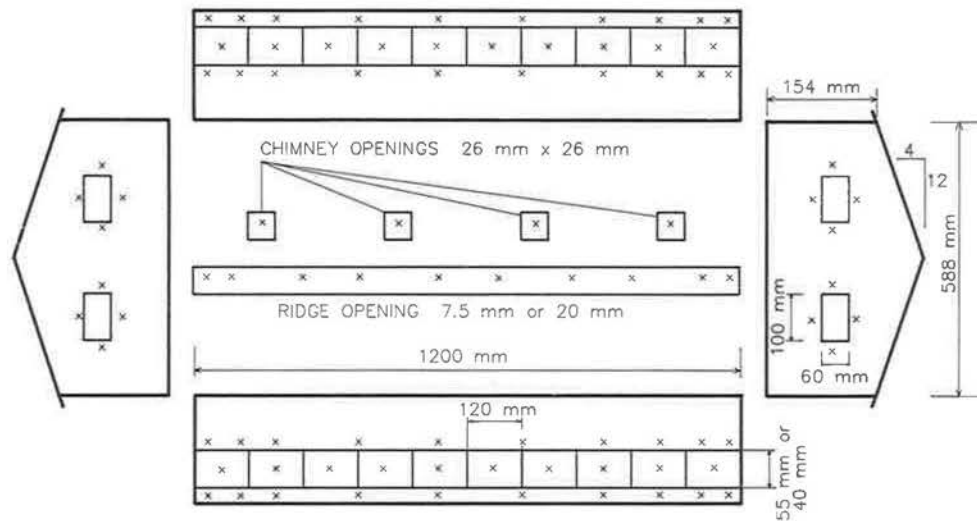


Figure 1 Scale model dimensions and tap locations for the sealed model.

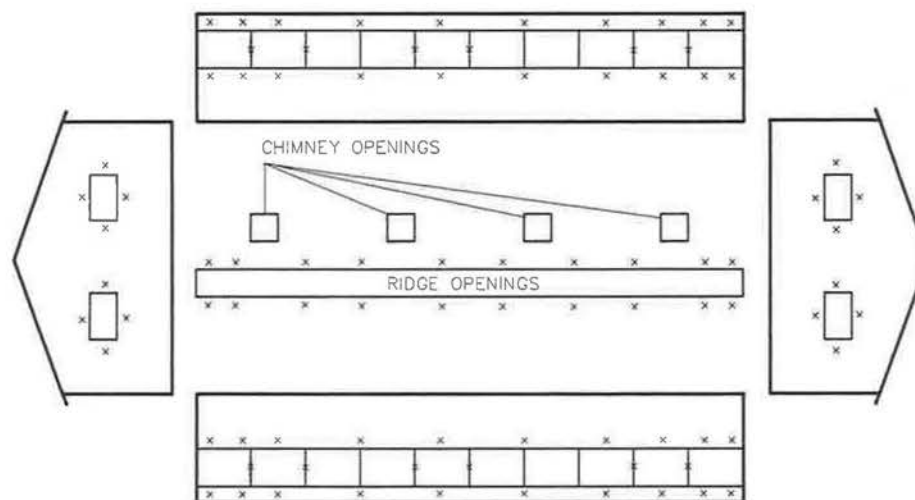


Figure 2 Tap locations for the open model.

due to partitions, 3 - perfect mixing was achieved, and 4 - the airflow was due to mean pressure differences alone and fluctuating pressure effects were ignored.

Theoretical estimates of airflow rates can be calculated using the external pressure distribution around an open or a sealed model [10,11] assuming that: 1 - the internal flow does not disturb the external pressure fields, 2 - the configuration of external wall openings and internal partitioning is known, and 3 - the flow rates through a given opening can be calculated from the following relationship.

$$Q_j = C_{dj} A_j V_{ref} \frac{C_{p_j} - C_{p_{in}}}{|C_{p_j} - C_{p_{in}}|^{1/2}} \quad (1)$$

where Q_j is the airflow through the opening, j, (m^3/s), C_{dj} is the discharge coefficient of the opening, j, the area of opening is A_j , (m^2), V_{ref} is the reference wind speed, (m/s), C_{p_j} is the pressure coefficient at the opening, j, and $C_{p_{in}}$ is the calculated internal pressure coefficient.

The sign associated with $(C_{p_j} - C_{p_{in}})$ determines the direction of the air flow at the j^{th} opening; positive implies inward and negative implies outward. The internal pressure coefficient is assumed to be uniform inside the ventilated air space [8,10,12]. Since the tests were performed for isothermal conditions, the inflow was equal to the outflow to satisfy continuity. The internal $C_{p_{in}}$ was determined by iteration using a computer.

External-internal pressure differences

A program was written in order to calculate and plot the ΔC_p values ($C_{p_j} - C_{p_{in}}$), using the calculated internal pressure coefficient. The directions of the arrows in Figs. 3 to 6 indicate the inflows or outflows of air. For all drawings, the length of the arrows are proportional to the magnitude of the pressure coefficient differences. It occasionally occurred that no arrows were plotted along the walls or the ridge, leaving a blank space; this indicated a zone where $\Delta C_p = 0$.

Measurement of internal pressures

According to various authors [10,12-14], the internal pressure coefficient, $C_{p_{in}}$, should remain uniform across the ventilated airspace. Based on these previous studies, only 10 taps were used to measure the internal pressure in the open scale model. However, during the wind tunnel tests, unexpected large variations in $C_{p_{in}}$ among these tap locations were recorded at various wind angles of incidence. Figure 7 presents the $C_{p_{in}}$ measurements tested with the open model, chimney, simulated 1100 mm sidewall with end wall openings.

Ventilation rate coefficients

In order to calculate the ventilation rate coefficients [10,11] for each test, the following formula was used:

$$C_{Q10} = \frac{Q}{V_{10} A_s} \quad (2)$$

The reference area of opening, A_s to use, differs among various authors. The total opening area on both sidewalls of the scale model is used [10,11] by some while

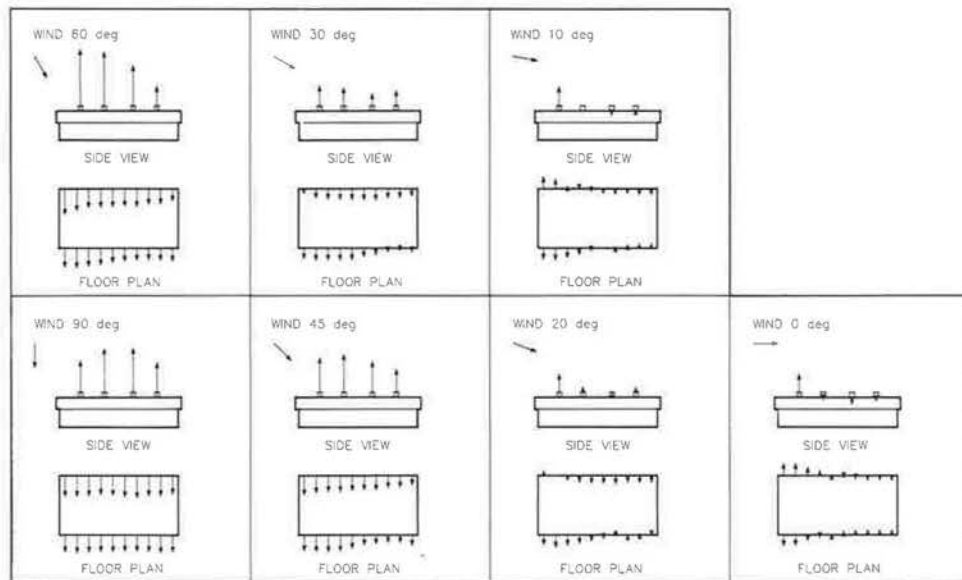


Figure 3 ΔC_{ps} (in-out), open model, chimney, simulated 800 mm sidewall openings, closed end walls, wind angles = 90°, 60°, 45°, 30°, 20°, 10° and 0°.

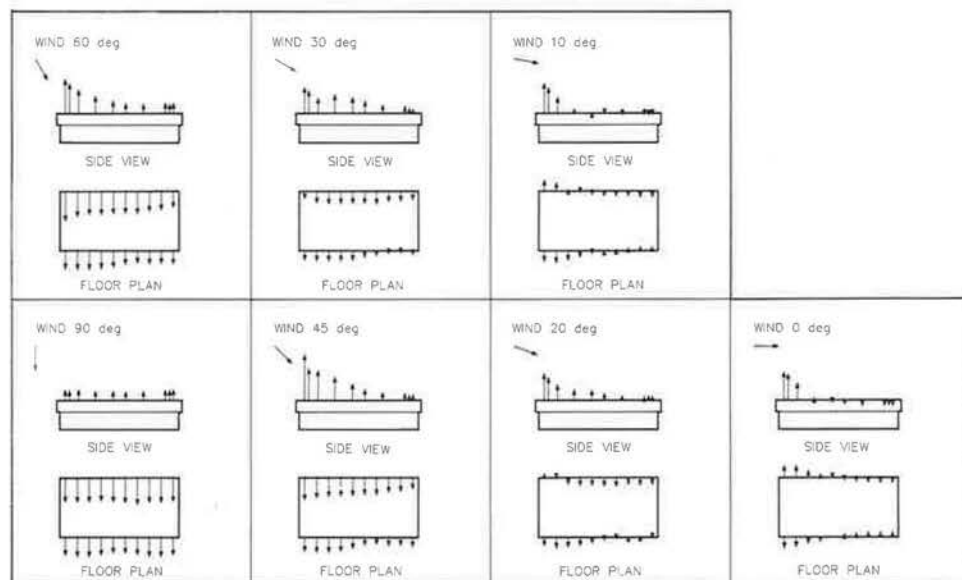


Figure 4 ΔC_{ps} (in-out), open model, simulated 150 mm ridge and 800 mm sidewall openings, closed end walls, wind angles = 90°, 60°, 45°, 30°, 20°, 10° and 0°.

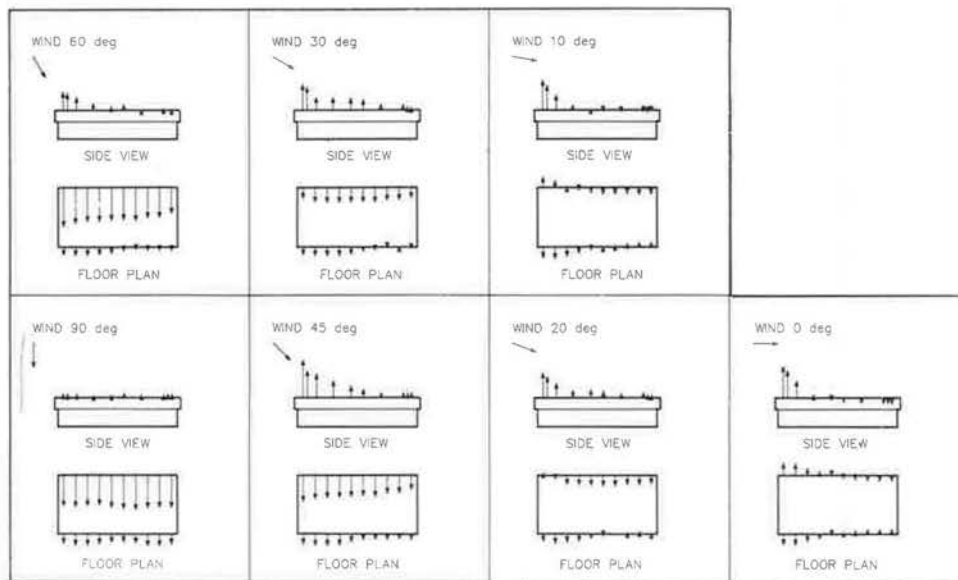


Figure 5 ΔC_{ps} (in-out), open model, simulated 400 mm ridge and 800 mm sidewall openings, closed end walls, 7 wind angles of incidence.

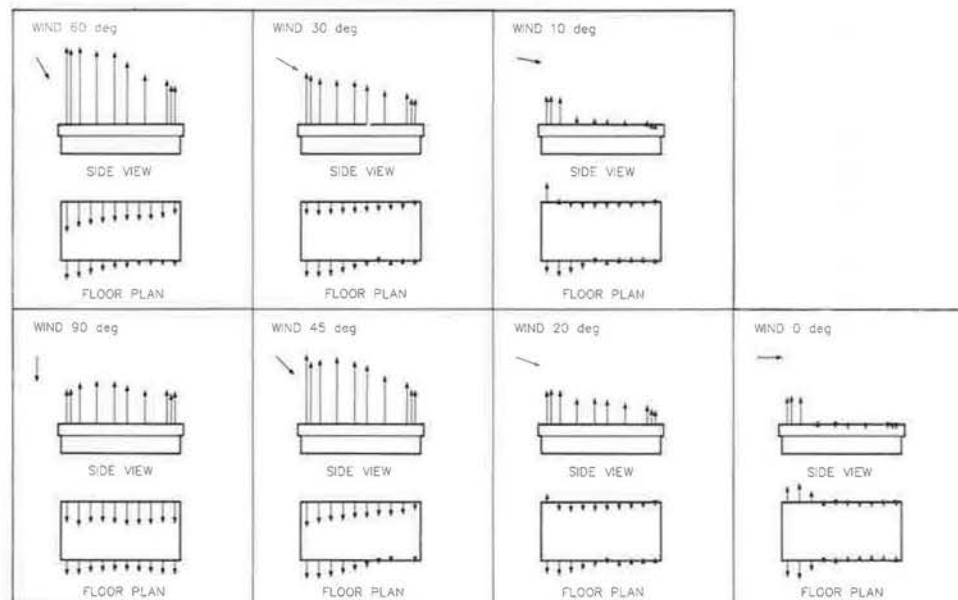


Figure 6 ΔC_{ps} (in-out), sealed model, simulated 150 mm ridge and 800 mm sidewall openings, closed end walls, wind angles = 90°, 60°, 45°, 30°, 20°, 10° and 0°.

it is common in agriculture to use only the frontal sidewall opening area [3,4]. For this study, the advantages for using only the frontal sidewall area as a reference opening were: 1 - visualization of the ridge's effects, 2 - visualization of the end wall openings' effects, and 3 - visualization of the respective sidewall opening areas' effects. All visualizations are in reference to the ventilation rate coefficients, C_{Q10} , at each wind angle of incidence.

RESULTS AND DISCUSSION

Figures 3 to 5 show the effect of various structural configurations on the airflow inlet and outlet zones, and on the variation of the magnitude of ΔC_p using an open model. Figure 6 shows predicted results based on a sealed model.

Effect of wind angles of incidence, open model

The results on the open model are used as the standard for comparison. Figure 3 presents the results for an open model with chimneys, simulated 800 mm sidewall openings, and closed end wall. At $\theta = 90^\circ$, ΔC_p s are uniform and positive over the windward surface, and uniform and negative on the leeward surface. The chimneys act as outlets. With $\theta = 45^\circ$ and 60° , the ΔC_p s uniformity disappears. This pressure distribution change was also reported by others [8,14]. At $\theta = 20^\circ$ and 30° , the wind pressure distributions at the leading edge of the building change. Flow reversal is observed near the end of the windward sidewall and the leeward sidewall. At $\theta = 0^\circ$ and 10° , air enters both sidewalls and exits at the upwind end. The leftmost chimney acts as an outlet while the other three act as inlets.

The qualitative observations of the zones of inlet-outlet made in another study on a similar scale model, and in a full scale swine barn, appear to be in agreement with the results presented here [1,2,7].

Effect of sidewall openings

Although not presented, the ΔC_p distribution with sidewall openings of 800 mm was similar to that obtained with sidewall openings of 1100 mm for all wind angles. A slight reduction in ΔC_p s was observed on the sidewall and the ridge with the larger sidewall openings. At $\theta = 90^\circ$, the ΔC_p s for the chimneys was greater with the 1100 mm sidewall opening than with the 800 mm sidewall opening.

Effect of end wall openings

It has been reported that the addition of end wall openings causes a slight reduction of ΔC_p s over both sidewalls, for $\theta = 45^\circ$, 60° and 90° [3,4]. At $\theta = 0^\circ$, 10° , 20° and 30° , the addition of the end wall openings did not change the inlet and outlet zones along the walls, however, the extra air entering the building reduced the ΔC_p s for both inlets and outlets, except near the leeward upwind end (highly negative zones), where ΔC_p s have increased.

Similar changes in the ΔC_p distributions were observed with larger ridge openings simulating 150 mm and 400 mm.

Effect of ridge openings

A comparison of Figs. 3 and 4 reveals similar ΔC_p distributions on the windward and leeward sidewalls using either chimneys or a 150 mm ridge. The major differences occur at the ridge where the ΔC_p s noted with the simulated 150 mm ridge opening is drastically reduced as compared to that noted with the chimneys for angles

from 30° to 90°. For $\theta = 0^\circ$, 10° and 20°, similar ΔC_p s are similar among the three ridge types.

The results of Figs. 4 and 5 indicate that an increase in the continuous ridge opening width causes a reduction in the ΔC_p over the ridge area, an increase in ΔC_p s for the inlet zones and a slight reduction in the ΔC_p s for the outlet zones.

Therefore, it can be concluded that a larger ridge opening does not change the ΔC_p distribution zones around the building except for: 1 - a slight increase of ΔC_p s over the inlet zones, 2 - a decrease of ΔC_p s over the outlet zones, and 3 - a decrease of ΔC_p s over the ridge opening.

Similar behavior was observed for the 1100 mm sidewall, with open end walls.

Sealed model

Based on Figure 6 and other data for a sealed model [3,4], an increase in the ridge width causes an increase in the ΔC_p s over the ridge. Also, different inlet and outlet zones between other sealed models with different ridge types were observed for $\theta = 0^\circ$, 10°, 20°, and 30°.

Open versus sealed models

The open versus sealed models with simulated 150 mm ridge, simulated 800 mm sidewall openings and closed end walls can be compared using Figs. 4 and 6. Similar inlet and outlet zones occur around the building walls. The open model data show higher ΔC_p s for the wall inlets and outlets, but the sealed model shows severe increases of ΔC_p s over the ridge area. For $\theta = 0^\circ$ to 20°, each model shows different wall inlet-outlet zones. As well, for $\theta = 20^\circ$ to 90°, each model shows different ΔC_p s for the ridge.

With a 400 mm ridge opening, and 1100 mm sidewall opening, drastic differences in the inlet-outlet zones are noticed for $\theta = 30^\circ$, 45° and 60° [3,4]. The sealed model predicts inflows at $\theta = 60^\circ$ over the leeward wall, while the open model predicts inflows at $\theta = 30^\circ$. The ΔC_p s over the ridge are also much higher with the sealed model for $\theta = 10^\circ$ to 90°, but similar for $\theta = 0^\circ$.

Generally, the comparisons of the results for the open model versus the sealed model indicate:

- 1 - Some differences in the ΔC_p s distributions around the building.
- 2 - A difference in ΔC_p magnitudes for inlet and outlet zones over the walls.
- 3 - A different ΔC_p with open end walls at $\theta = 90^\circ$, and also flow reversal at $\theta = 0^\circ$ and 10°.
- 4 - For all ridge opening configurations, the sealed model would over-predict the airflow through the ridge openings as compared to the open model.

These observations are consistently accentuated for the larger sidewall openings of 1100 mm versus 800 mm, which would lead one to believe that the larger the total opening area is, the larger the discrepancies in ΔC_p s between the open and sealed model.

Open model, measured internal pressure coefficients

Figure 7 presents the $C_{p_{in}}$ measurements over the sidewall area (floor plan) and the roof (roof plan). Large variations in $C_{p_{in}}$ are recorded. For example, at $\theta = 30^\circ$, the lowest $C_{p_{in}}$ equals -0.23 while the highest is 0.06, a $C_{p_{in}}$ variation of 0.29 across the airspace. The largest $C_{p_{in}}$ variations are noted for $\theta = 90^\circ$ to 30°.

$C_{p_{in}}$ associated with airflow patterns

For naturally ventilated buildings with large openings, internal air speeds vary between 0.1 to 0.6 times the reference wind speed for winds parallel and perpendicular to the building, respectively [8]. The reported inside airflow patterns for a similar model [1,2] suggest that the changes in airflow directions due to the interior building design associated with the inlet and exhaust of air by the various openings may create changes of the interior wind speeds thus, modifying the $C_{p_{in}}$ values across the model's inner airspace. The close relationship between the inside floor and roof airflow patterns and the $C_{p_{in}}$ variations are remarkable [3].

Detailed studies are needed to evaluate the number of interior pressure taps required and their locations in order to obtain an accurate picture of the $C_{p_{in}}$ variations inside naturally ventilated buildings with large continuous sidewall, ridge or chimney, and end wall openings. Based on the measured internal pressures, the following comments can be made: 1 - large 3-dimensional $C_{p_{in}}$ variation should be anticipated inside these types of naturally ventilated buildings, 2 - the previously observed and reported airflow patterns seems to coincide with the gradients of $C_{p_{in}}$, and 3 - the six taps installed at the roof level and the four taps mounted over the sidewall would be a minimum to use for the analysis of internal pressure.

Calculated versus measured $C_{p_{in}}$

Additional observations on the effects of the two sidewall area sizes, the open or closed end walls and the three ridge openings [3] tend to show:

- 1 - The differences between the calculated and the average of the measured $C_{p_{in}}$ were small with the chimney and 150 mm ridge, but larger with the 400 mm ridge.
- 2 - For the 800 mm versus the 1100 mm sidewall opening with open or closed end walls, some differences in $C_{p_{in}}$ were recorded at $\theta = 90^\circ$ and 60° , for both the 150 mm and 400 mm ridges.
- 3 - The distributions of the $C_{p_{in}}$ were more uniform through the building when the end walls were open.
- 4 - The variations in $C_{p_{in}}$ inside the building may produce local effects on the air inlet and outlet zones as well as on the ventilation rate. Sufficient data are not available to be able to study the effects of the variation of $C_{p_{in}}$ on local and total ventilation rates.

Ventilation rate coefficients - Open model general observations

Figure 8 shows the variation of the ventilation rate coefficient with the wind angles of incidence for the chimney, 150 mm and 400 mm ridge openings. The results predict a 50% reduction in the ventilation rate when the wind is parallel as compared to perpendicular to the building.

Generally, the C_{Q10} curves have similar shapes with the maximum C_{Q10} value at $\theta = 90^\circ$, the minimum value at $\theta = 10^\circ$, and the largest drop in C_{Q10} between $\theta = 45^\circ$ and 20° . Although not shown, C_{Q10} was also influenced by the size of the sidewall opening [3].

Figure 8 shows that the use of the larger ridge opening produces higher ventilation rate coefficients. There is little difference between the C_{Q10} values for the chimney and the 150 mm ridge. The use of end wall openings also seems to

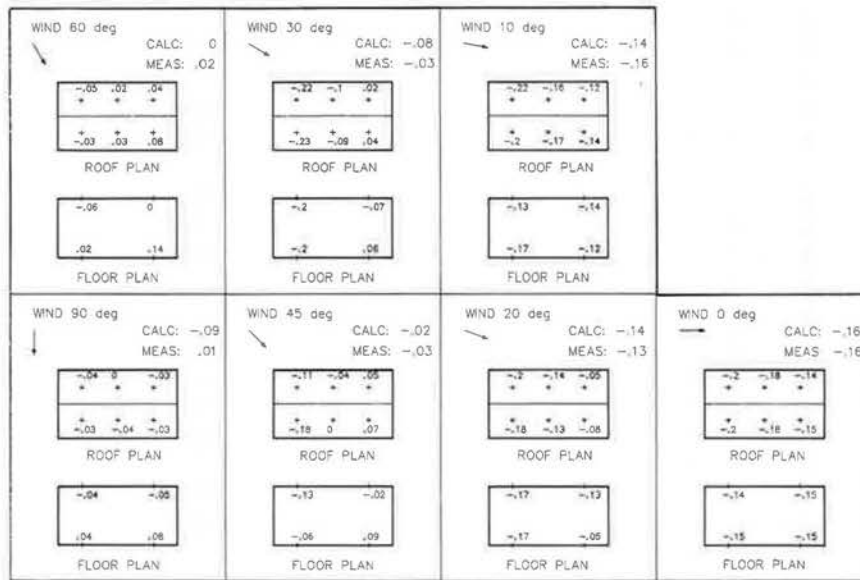


Figure 7 Measured $C_{p,ib}$, open model, chimney, simulated 1100 mm sidewall openings, open end walls, wind angles = 90°, 60°, 45°, 30°, 20°, 10° and 0°.

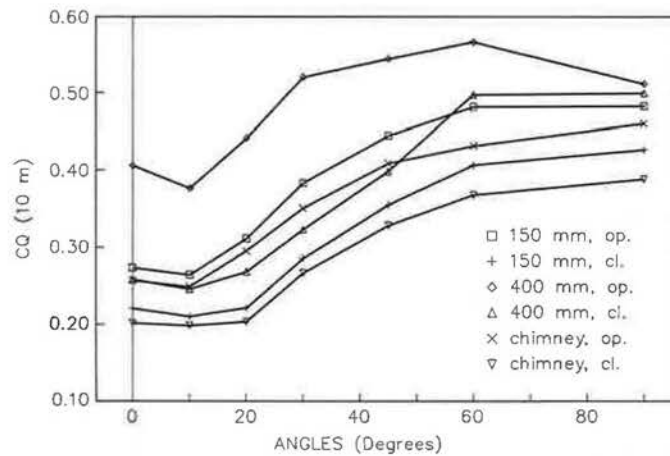


Figure 8 Open model, comparison among chimney, simulated 150 mm and 400 mm ridges with simulated 800 mm sidewall.

substantially increase the C_{Q10} values for all wind angles.

In a case where the ventilation rates would have to be increased, the designers would have to evaluate the cost/benefits of enlarging sidewall, end wall or ridge openings.

Open versus sealed model

Although not shown here, there were differences noted between the C_{Q10} values obtained using the open or sealed model for the same buildings [3].

The open model C_{Q10} values with the chimney and 150 mm ridge were higher than the sealed model values for $\theta = 90^\circ$ to 30° and lower for $\theta = 20^\circ$ to 0° . The differences were generally greater when the ridge opening was increased from the chimney to the 400 mm ridge width.

These differences of open versus sealed model C_{Q10} values would lead one to believe that the larger the total opening area is on the sidewalls, end walls, and ridge, the larger the discrepancies in C_{Q10} values will be.

SUMMARY AND CONCLUSION

Comparisons between the open and sealed models were based on graphical representations of the measured and calculated internal pressure coefficients, $C_{p_{in}}$, local external-internal pressure differences, ΔC_p s and the ventilation rate coefficients, C_{Q10} , for all building configurations.

A total of 105 tests were done with open and sealed models. The model was transformed in order to study the following structural parameters: 1 - three ridge opening configurations consisting of intermittent chimneys, simulated 150 mm or 400 mm wide continuous ridge openings, 2 - two sidewall opening areas, simulating 800 mm or 1100 mm high continuous sidewall openings, and 3 - the use of two end wall openings.

Each building configuration was investigated for seven wind angles of incidence.

From the results, it could be inferred that:

- 1 - Changing the building sidewall, end wall or ridge opening in function of the wind angles of incidence had an effect on the ΔC_p distributions around the building, the measured and calculated $C_{p_{in}}$, and the ventilation rate coefficients C_{Q10} for all wind angles.
- 2 - Large 3-dimensional $C_{p_{in}}$ variations should be anticipated inside open scale models for these types of naturally ventilated buildings.
- 3 - For all types of ridge openings, the sealed model show considerably higher ΔC_p s along the ridge and lower ΔC_p s over the leeward wall as compared to the open model.
- 4 - The larger the total opening area on the sidewall, end wall and ridge, the larger the discrepancies will be between the results of the open and sealed models for ΔC_p s, $C_{p_{in}}$ and C_{Q10} .

For future research work on naturally ventilated buildings with large sidewall, end wall and ridge opening areas, it appears that the use of open models should be recommended because of the reported large 3-dimensional $C_{p_{in}}$ variations within the open model and the different external pressure coefficients measured with various structural building configurations.

Acknowledgement

The authors gratefully acknowledge the research officers of the Applied Aerodynamics Laboratory, National Research Council of Canada for their extensive and helpful contribution during this study.

The financial support provided by the Ontario Ministry of Agriculture and Food, Agriculture Canada, Ontario Hydro, the Canadian Electrical Association and the Ontario Pork Producers' Marketing Board was greatly appreciated.

REFERENCES

- 1 Choinière, Y., Blais, F. and Munroe, J.A., *Can. Agric. Eng.*, (1988), Vol. 30(2), pp. 293-297.
- 2 Choinière, Y., Munroe, J.A., Dubois, H., Desmarais, G., Larose, D. and Blais, F., *Can. Soc. of Agric. Eng.*, (1988), Paper No. 88-113, 151 Slater St., Ottawa, Ont.
- 3 Choinière, Y., "Wind induced natural ventilation of low-rise buildings for livestock housing by the pressure difference method and concentration decay method", M.Sc. thesis, Un. of Ottawa, Dept. of Civil Eng., Canada, (1991), 491 pp.
- 4 Choinière, Y., Munroe, J.A., Tanaka, H., Suchorski-Tremblay, A. and Tremblay, S., *Can. Soc. of Agric. Eng.*, (1990), Paper No. 90-124, 151 Slater St., Ottawa, Ont.
- 5 Cermak, J.E., Poreh, M., Peterka, J.A. and Ayad, S.S., *J. of Transp. Eng.*, (1984) Vol. 110(1), pp. 67-79.
- 6 Choinière, Y., Munroe, J.A., Desmarais, G., Renson, Y. and Ménard, O., *Can. Soc. of Agric. Eng.*, (1988), Paper No. 88-115, 151 Slater St., Ottawa, Ont.
- 7 Choinière, Y., Munroe, J.A., Desmarais, G., Dubois, H. and Renson, Y., *Am. Soc. of Agric. Eng.*, (1989), CSAE-ASAE Paper No. 89-4065, St-Joseph, MI 49085 USA
- 8 Aynsley, R.M., Melbourne, W. and Vickery, B.J. *Applied Sc. Pub. Ltd.*, London, (1977), 254 pp.
- 9 Holmes, J.D., *Commonwealth Sci. and Ind. Res. Org.*, Div. of Bldg Res., Australia, (1983), 91 pp.
- 10 Vickery, B.J., Baddour, R.E. and Karakatsanis, C., Report No. BLWT-SS2-1983, Un. of Western Ont., London, Ont., N6A 5B9, (1977), 90 pp.
- 11 Vickery B.J. and Karakatsanis, C., *ASHRAE Trans.*, (1987), Vol. 93(2), pp. 2198-2213.
- 12 Vickery, B.J., *J. of Wind Eng. and Ind. Aero.*, (1986), Vol. 23, pp. 259-271.
- 13 Stathopoulos, T., Surry, D. and Davenport, A.G., *Proc. of the Fifth Intl. Conf. of Wind Engng.*, Pergamon Press, (1979), Vol. 1, p. 451-463.
- 14 Davenport, A.G., Surry, D. and Stathopoulos, T., Report No. BLWT-SS8-1977, Un. of Western Ont., London, Ont., N6A 5B9, (1977), 74 pp.